Improved impact-parameter method for electronic excitation and dissociation of diatomic molecules by electron impact

Michael J. Redmon, Bruce C. Garrett, Lynn T. Redmon, and C. W. McCurdy*
Chemical Dynamics Corporation, 1550 West Henderson Road, Columbus, Ohio 43220
(Received 26 December 1984)

The impact-parameter method for electron-impact excitation of diatomic molecules is reformulated to explicitly treat molecular vibration and rotation and to permit the study of molecular dissociation. Applications are made to optically allowed transitions involving the $X\,^1\Sigma_g^+$, $B\,^1\Sigma_u^+$, and $B'\,^1\Sigma_u^+$ states of H_2. The resulting cross sections are compared to other theoretical calculations and to experimental data. This method is applicable to heavy diatomic molecules and is expected to be useful in studying trends in electronic excitation and dissociation cross sections associated with variations in internal energy.

I. INTRODUCTION

Processes involving electron-molecule collisions are important in gas-laser systems, atmospheric physics, and photochemistry. Because of their importance in laser plasmas,[1] collision-induced electronic excitations and dissociation by electron impact have been the subject of recent experimental interest;[2] however, there has been less progress in the theoretical description of these processes. Although electron-molecule scattering theory has been significantly advanced in the areas of elastic scattering and rotational and vibrational excitation,[3–5] the *ab initio* calculation of electronic excitation of molecules by electron impact is relatively new. Early work in this area includes Born or other "plane-wave" approximation calculations[6–15] that are reliable only at relatively high energies. In addition a two-state close-coupling method[16–18] has been applied to electronic excitation and dissociation of a number of states of H_2 and to the excitation of the $a\,^1\Pi_g$ state of N_2.[19] In these calculations electron exchange is correctly included, but the treatment of nuclear motion utilizes the Franck-Condon approximation. The theory can treat both singlet-singlet and singlet-triplet transitions. The distorted-wave Born approximation employing the L^2 T-matrix[20–26] or R-matrix[27] methods has also received attention. Most applications of the distorted-wave methods have been to processes involving excited electronic states of H_2, although applications to N_2 (Ref. 24) and F_2 (Ref. 25) have also been made. The method is most applicable to spin-forbidden transitions involving short-range interactions.

Hazi has extended the semiclassical impact-parameter method[28,29] to electronic excitation of diatomic molecules.[30,31] The formulation neglects exchange, and is best suited for the treatment of optically allowed transitions that require many partial waves in conventional close-coupling or distorted-wave theories. Thus it is complementary to these approaches and to the high-energy Born-type approximations. In the semiclassical impact-parameter (IP) method the motion of the electrons (including the incident electron) is separated from nuclear motion by the Born-Oppenheimer approximation. This allows the molecular electronic problem to be treated as accurately as necessary, independently of the scattering. Hazi's theory assumes degenerate rotational states and averages the transition probability over molecular orientations. His formulation results in cross sections that satisfy reciprocity, and this represents a refinement over the original impact-parameter method. However, the Franck-Condon approximation is utilized, and internuclear distances are treated as static. Thus vibrational and rotational motion are neglected. Because of these approximations in Hazi's theory, the resulting cross sections do not distinguish between bound (rovibrational) and unbound (continuum) channels. When the method is extended to include nuclear motion, this differentiation can be made.

In Sec. II we present extensions of the impact-parameter model to include the effects of initial vibrational and rotational excitation upon electron-impact-induced excitation and dissociation. We are interested in nonresonant optically allowed electronic excitations of diatomic molecules. These involve dipole-allowed spin-conserving transitions. These excitations can be to bound rovibrational levels of the final electronic state or to parts of the potential-energy curve above the dissociative limit of the final electronic state. We consider only processes of direct dissociation through excited electronic states rather than the resonance-enhanced dissociative attachment process. When the diatomic molecule is treated as a symmetric top, electronic and rotational angular momentum are coupled; however, the resulting cross section retains a separability of structural and dynamical factors analogous to that of Hazi's original method and involves simple products of Clebsch-Gordon coefficients. By performing suitable averages, the original cross-section formula of Hazi is obtained.

Section III provides the relevant computational details, while Sec. IV presents the results of the cross-section calculations for several levels of approximation within the IP method. As a test of the method for electronic excitation to bound vibrational states, we apply the IP method to the $X\,^1\Sigma_g^+$ to $B\,^1\Sigma_u^+$ and $X\,^1\Sigma_g^+$ to $B'\,^1\Sigma_u^+$ transitions in H_2 and compare with previous experimental[32] and theoreti-

cal[15,16,23,26,30] studies. We also apply it to the direct dissociation of $H_2(^1\Sigma_g^+)$ through the $B'\,^1\Sigma_u^+$ state and compare the results with experimental[33,34] and theoretical[12,26] studies. Section V provides a summary and the conclusions.

II. THEORY

Hazi's implementation of the impact-parameter method employs the "fixed-nuclei" approximation,[4] averaging the semiclassical transition probability[30]

$$P_{fi}=g_i^{-1}\sum_{\lambda_i=\pm\Lambda_i}\sum_{\lambda_f=\pm\Lambda_f}\left|\hbar^{-1}\int_{-\infty}^{\infty}dt\,e^{i\Delta E_{fi}t/\hbar}V_{fi}(t)\right|^2 \tag{1}$$

over all molecular orientations. In this expression g_i is the degeneracy of the initial electronic state, Λ_i and Λ_f are the usual projections of electronic angular momentum on the body-fixed axis, ΔE_{fi} is the transition energy, and $V_{fi}(t)$ is the time-dependent matrix element of the perturbation. We present an extension of the theory to allow treatment of those processes that require consideration of nuclear motion.

We work within the framework of the adiabatic nuclei approximation[35] and employ a Born-Oppenheimer factorization of the wave function for the target molecule

$$\Psi_{\alpha v\lambda}^{jm}(\underset{\sim}{x};\mathbf{R})=\psi_{\alpha\lambda}(\underset{\sim}{x};R)\chi_{vj}^{\alpha}(R)N_{m\lambda}^{j}(\hat{\mathbf{R}})\ . \tag{2}$$

The function $\psi_{\alpha\lambda}$ represents an approximate solution (for electronic state α) to the n-electron Schrödinger equation for the electrons in the molecule moving in the field of the "fixed" nuclei, χ_{vj}^{α} is the vibrational wave function for the (v,j) rovibrational level of electronic state α, and $N_{m\lambda}^{j}$ is a symmetric-top function for a diatomic molecule with electronic angular momentum component λ.[36] In our notation, $\underset{\sim}{x}$ collectively represents the coordinates of the target electrons, while R and $\hat{\mathbf{R}}$ represent the magnitude and angular position of the relative position vector $\mathbf{R}$. All target electronic coordinates are referred to the body-fixed (BF) frame and the polar z axis is taken along the line joining the nuclei ($\hat{\mathbf{R}}$).

The vibrational wave functions for electronic state α are orthonormal eigenfunctions of the equation

$$[-(\hbar^2/2\mu_{AB})d^2/dR^2+V_{\alpha}(R)+\hbar^2 j(j+1)/2\mu_{AB}R^2]\chi_{vj}^{\alpha}(R)=\varepsilon_{vj}^{\alpha}\chi_{vj}^{\alpha}(R)\ , \tag{3}$$

where μ_{AB} is the reduced mass of the diatomic molecule, $\varepsilon_{vj}^{\alpha}$ is the vibrational energy level, and $V_{\alpha}(R)$ is the potential energy curve for electronic state α.

The symmetric-top functions are represented in terms of Wigner D functions[37]

$$N_{m\lambda}^{j}(\hat{\mathbf{R}})=\left[\frac{2j+1}{8\pi^2}\right]^{1/2}[D_{m\lambda}^{j}(\hat{\mathbf{R}})]^*\ , \tag{4}$$

where the projectile electron is assumed to be initially moving along the spaced-fixed (SF) Z axis, and where $\hat{\mathbf{R}}$ represents the two (nontrivial) Euler angles relating the BF frame to SF axes. This normalization assumes integration over all three Euler angles.

In our formulation of the semiclassical impact-parameter method, the projectile-electron velocity is assumed to be high enough that the collision time is short compared to the periods of molecular vibration or rotation. Then the adiabatic nuclei approximation is expected to be valid, and the time-dependent perturbation matrix element required in Eq. (1) is obtained by taking the matrix element of the projectile-target interaction between initial and final molecular states represented in the form of Eq. (2). If $\mathbf{r}'(t)$ represents the classical trajectory of the projectile electron, and $\mathbf{r}_q'$ the coordinates of a target electron (the primes indicate SF coordinates), then this matrix element can be expressed as

$$V_{fi}(t)=\int d\underset{\sim}{x}\int dR\,R^2\int d\hat{\mathbf{R}}\,\psi_{\alpha_f\lambda_f}^{*}(\underset{\sim}{x};R)R^{-1}[\chi_{v_fj_f}^{\alpha_f}(R)]^*[N_{m_f\lambda_f}^{j_f}(\hat{\mathbf{R}})]^*\sum_{q=1}^{n}\frac{e^2}{|\mathbf{r}'(t)-\mathbf{r}_q'|}\psi_{\alpha_i\lambda_i}(\underset{\sim}{x};R)R^{-1}\chi_{v_ij_i}^{\alpha_i}(R)N_{m_i\lambda_i}^{j_i}(\hat{\mathbf{R}})\ . \tag{5}$$

To evaluate this expression, we use the usual multipole expansion[38]

$$|\mathbf{r}'(t)-\mathbf{r}_q'|^{-1}=\sum_{l=0}^{\infty}\sum_{\mu=-l}^{+l}\left[\frac{4\pi}{2l+1}\frac{r_<^l}{r_>^{l+1}}Y_{l\mu}^{*}(\hat{\mathbf{r}}')Y_{l\mu}(\hat{\mathbf{r}}_q')\right]\ , \tag{6}$$

where $r_<$ ($r_>$) is the lesser (greater) of r' and r_q'. We keep only the asymptotic ($r'>r_q'$) terms of this expansion because the impact-parameter treatment is valid only for collisions that do not penetrate the electron cloud of the target.[30] We are presently interested only in optical (dipole-allowed) transitions (for which the dominant contribution is from $l=1$). Therefore, we approximate the electron-target interaction by

$$|\mathbf{r}'(t)-\mathbf{r}_q'|^{-1}\simeq\frac{4\pi}{3}\sum_{\mu=-1}^{+1}\frac{r_q'}{(r')^2}Y_{1\mu}^{*}(\hat{\mathbf{r}}')Y_{1\mu}(\hat{\mathbf{r}}_q')\ . \tag{7}$$

Since the electron coordinates of the electronic wave functions employed in the matrix element V_{fi} given by Eq. (5) are expressed in BF coordinates, Eq. (7) must be transformed to BF coordinates before the integration can be carried out. Using the Wigner rotation matrices,[39] we obtain

$$|\mathbf{r}'(t)-\mathbf{r}_q'|^{-1}\simeq\frac{4\pi}{3}\sum_{\mu=-1}^{+1}\sum_{m=-1}^{+1}\frac{r_q}{(r')^2}Y_{1\mu}^{*}(\hat{\mathbf{r}}')[D_{\mu m}^{1}(\hat{\mathbf{R}})]^*Y_{1m}(\hat{\mathbf{r}}_q)\ . \tag{8}$$

Substituting this expression into Eq. (5), we note that the part of the resulting expression involving integration over the target-electron coordinates is the matrix element of the spherical representation of the dipole operator. This operator is a spherical tensor of rank 1, so (from the Wigner-Eckart theorem[37]) we have

$$\sum_{m=-1}^{+1}[D^1_{\mu m}(\hat{\mathbf{R}})]^* \int d\underset{\sim}{x}\,\psi^*_{\alpha_f\lambda_f}(\underset{\sim}{x};R)\sum_{q=1}^{n} e r_q Y_{1m}(\hat{\mathbf{r}}_q)\psi_{\alpha_i\lambda_i}(\underset{\sim}{x};R)=\left[\frac{3}{4\pi}\right]^{1/2}[D^1_{\mu\Delta\lambda}(\hat{\mathbf{R}})]^* M_{\alpha_f\alpha_i}(R)\,, \tag{9}$$

where the electronic transition dipole moment is

$$M_{\alpha_f\alpha_i}(R)=\left|\int d\underset{\sim}{x}\,\psi^*_{\alpha_f\lambda_f}(\underset{\sim}{x};R)\sum_{q=1}^{n} e\mathbf{r}_q\psi_{\alpha_i\lambda_i}(\underset{\sim}{x};R)\right| \tag{10}$$

and $\Delta\lambda=\lambda_f-\lambda_i$. The transition matrix element can now be written as

$$V_{fi}(t)\simeq\left[\frac{4\pi}{3}\right]^{1/2} eM^{\alpha_f\alpha_i}_{v_fj_fv_ij_i}\sum_{\mu=-1}^{+1}\frac{1}{(r')^2}Y^*_{1\mu}(\hat{\mathbf{r}}')\int d\hat{\mathbf{R}}[N^{j_f}_{m_f\lambda_f}(\hat{\mathbf{R}})]^*[D^1_{\mu\Delta\lambda}(\hat{\mathbf{R}})]^* N^{j_i}_{m_i\lambda_i}(\hat{\mathbf{R}})\,, \tag{11}$$

where the electronic transition dipole moment is averaged over the initial and final vibrational wave functions

$$M^{\alpha_f\alpha_i}_{v_fj_fv_ij_i}=\int_0^\infty dR[\chi^{\alpha_f}_{v_fj_f}(R)]^* M_{\alpha_f\alpha_i}(R)\chi^{\alpha_i}_{v_ij_i}(R)\,. \tag{12}$$

For the remaining integral over Euler angles, we use the Wigner D-function representation of the symmetric-top wave functions, Eq. (4),

$$\begin{aligned} I_R&=\left[\frac{2j_f+1}{8\pi^2}\right]^{1/2}\left[\frac{2j_i+1}{8\pi^2}\right]^{1/2}\int d\hat{\mathbf{R}}\,D^{j_f}_{m_f\lambda_f}(\hat{\mathbf{R}})[D^1_{\mu\Delta\lambda}(\hat{\mathbf{R}})]^*[D^{j_i}_{m_i\lambda_i}(\hat{\mathbf{R}})]^* \\ &=(-1)^{m_i-\lambda_i}\left[\frac{2j_f+1}{8\pi^2}\right]^{1/2}\left[\frac{2j_i+1}{8\pi^2}\right]^{1/2}\int d\hat{\mathbf{R}}\,[D^1_{\mu\Delta\lambda}(\hat{\mathbf{R}})]^* D^{j_f}_{m_f\lambda_f}(\hat{\mathbf{R}})D^{j_i}_{-m_i-\lambda_i}(\hat{\mathbf{R}})\,, \end{aligned} \tag{13}$$

where we have used the property[39]

$$[D^{j_i}_{m_i\lambda_i}(\hat{\mathbf{R}})]^*=(-1)^{m_i-\lambda_i}D^{j_i}_{-m_i-\lambda_i}(\hat{\mathbf{R}})\,. \tag{14}$$

Making use of the integral theorem for the product of three rotation matrices,[39] we obtain

$$I_R=(-1)^{m_i-\lambda_i}\frac{(2j_f+1)^{1/2}(2j_i+1)^{1/2}}{8\pi^2}\frac{2}{3}\delta_{m_f-m_i,\mu}C(j_i,j_f,1;-m_i,m_f)C(j_i,j_f,1;-\lambda_i,\lambda_f)\,. \tag{15}$$

We have now reduced the rotational factor to a simple expression involving the product of two Clebsch-Gordan coefficients. The time-dependent perturbation matrix element now becomes

$$\begin{aligned} V_{fi}(t)\simeq\frac{2}{3}\left[\frac{4\pi}{3}\right]^{1/2} e\frac{(2j_f+1)^{1/2}(2j_i+1)^{1/2}}{8\pi^2}(-1)^{m_i-\lambda_i}M^{\alpha_f\alpha_i}_{v_fj_fv_ij_i}C(j_i,j_f,1;-m_i,m_f)C(j_i,j_f,1;-\lambda_i,\lambda_f) \\ \times\frac{1}{(r')^2}\sum_{\mu=-1}^{+1}\delta_{m_f-m_i,\mu}Y^*_{1\mu}(\hat{\mathbf{r}}')\,. \end{aligned} \tag{16}$$

Substituting Eq. (16) into (1), summing over final angular momenta (electronic and rotational), and averaging over initial angular momenta results in the following form for the transition probability:

$$\begin{aligned} P^{\alpha_f\alpha_i}_{v_fj_fv_ij_i}(t)=\frac{2j_f+1}{27g_i}\left[\frac{e^2}{\hbar^2}\right]|M^{\alpha_f\alpha_i}_{v_fj_fv_ij_i}|^2\left|\int_{-\infty}^{\infty}dt\exp(i\,\Delta E_{fi}\,t/\hbar)\frac{r'(t)}{(r')^3}\right|^2 \\ \times\sum_{\lambda_f=\pm\Lambda_f}\sum_{\lambda_i=\pm\Lambda_i}|C(j_i,j_f,1;-\lambda_i,\lambda_f)|^2\sum_{m_f=-j_f}^{j_f}\sum_{m_i=-j_i}^{j_i}|C(j_i,j_f,1;-m_i,m_f)|^2\,. \end{aligned} \tag{17}$$

We have also used the relation defining the displacement vector in terms of the spherical harmonics[39]

$$\sum_{\mu=-1}^{+1} r'Y^*_{1\mu}(\hat{\mathbf{r}}')\hat{\mathbf{e}}_\mu=\left[\frac{3}{4\pi}\right]^{1/2}r' \tag{18}$$

to simplify the time-dependent integral.[30] This form for the probability results from the present restriction to dipole-allowed transitions. Thus even with the inclusion of vibrational and rotational degrees of freedom, we still obtain a form analogous to Hazi's, i.e., a factorization of the transition probability into the product of a dynamical factor depending on projectile-electron coordinates (classical trajectory) and a unitless structural factor depending only upon properties of the target molecule.[30]

The structural factor is written as

$$S^{\alpha_f\alpha_i}_{v_f j_f v_i j_i}=\frac{m_e^2e^2}{\hbar^4}\frac{2j_f+1}{27g_i}\,|M^{\alpha_f\alpha_i}_{v_f j_f v_i j_i}|^2\sum_{\lambda_f=\pm\Lambda_f}\sum_{\lambda_i=\pm\Lambda_i}|C(j_i,j_f,1;-\lambda_i,\lambda_f)|^2\sum_{m_f=-j_f}^{+j_f}\sum_{m_i=-j_i}^{+j_i}|C(j_i,j_f,1;-m_i,m_f)|^2\,, \tag{19}$$

where m_e is the electron mass. It contains Clebsch-Gordan coefficients that impose optical selection rules due to the requirements of the triangle inequality.[38] The structural factor is zero unless $j_f=j_i\pm1$. It also vanishes when $|\Delta\Lambda|>1$, and so we can have $\Sigma\leftrightarrow\Sigma$, $\Sigma\leftrightarrow\Pi$, and $\Pi\leftrightarrow\Pi$ transitions but not $\Sigma\leftrightarrow\Delta$. Extending the present theory to permit the description of higher-order processes would require including additional terms in the multipole expansion of the electron-target interaction. If we assume degenerate rotational states, the structural factor reduces to

$$S^{\alpha_f\alpha_i}_{v_f v_i}=\frac{m_e^2e^2}{3g_i\hbar^4}(2-\delta_{\Lambda_f,0})(2-\delta_{\Lambda_i,0})\,|M^{\alpha_f\alpha_i}_{v_f v_i}|^2\,. \tag{20}$$

Evaluation of the dynamical factor follows the derivation of Hazi exactly. By assuming that the trajectories for the incident electron are straight lines and energy exchange with the target occurs at the distance of closest approach and requiring conservation of energy and angular momentum, the dynamical factor can be expressed in terms of modified Bessel functions[40] $K_i(\gamma)$ and modified Struve functions[40] $S_i(\gamma)$. The derivation is found in Hazi's paper,[30] and we present only the final result integrated over the impact parameter:

$$\begin{aligned}D^{\alpha_f\alpha_i}_{v_f j_f v_i j_i}(E)=\frac{2\pi\hbar^2}{m_e^2u_i^2}\Big[&\gamma_iK_0(\gamma_i)K_1(\gamma_i)+\gamma_fK_0(\gamma_f)K_1(\gamma_f)-\tfrac{1}{4}\pi^2[\gamma_iS_0(\gamma_i)S_1(\gamma_i)+\gamma_fS_0(\gamma_f)S_1(\gamma_f)]\\&+\bar\gamma\{K_1(\gamma_f)K_0(\gamma_i)+K_0(\gamma_f)K_1(\gamma_i)+\tfrac{1}{4}\pi^2[S_0(\gamma_i)S_1(\gamma_f)+S_1(\gamma_i)S_0(\gamma_f)]\}\\&+(u_i^2-u_f^2)(u_i^2+u_f^2)^{-1}\left[\ln(\gamma_f/\gamma_i)+\tfrac{1}{2}\pi\int_{\gamma_i}^{\gamma_f}d\gamma\,S_0(\gamma)\right]\Big]\,,\end{aligned} \tag{21}$$

where

$$m_eu_i^2=E\,, \tag{22}$$

$$m_eu_f^2=E-\Delta E\,, \tag{23}$$

$$\gamma_i=l_0\,\Delta E/m_eu_i^2\,, \tag{24}$$

$$\gamma_f=l_0\,\Delta E/m_eu_f^2\,, \tag{25}$$

$$\bar\gamma=2l_0\,\Delta E/m_e(u_i^2+u_f^2)\,, \tag{26}$$

E is the relative translational energy of the incident electron, m is the electron mass, l_0 is the minimum value of the incident electronic-orbital angular momentum quantum number, u_i (u_f) is the initial (final) electron speed, and the transition energy ΔE is defined by

$$\Delta E=\varepsilon^{\alpha_f}_{v_f j_f}-\varepsilon^{\alpha_i}_{v_i j_i}\,. \tag{27}$$

The dependence of the dynamical factor on molecular vibrational and rotational quantum numbers is only through the transition energy.

The cross section is expressed as the product of the structural factor for the molecule, given by Eq. (19), and the dynamical factor for the electron, given by Eq. (21):

$$\sigma^{\alpha_i\alpha_f}_{v_i j_i v_f j_f}(E)=S^{\alpha_f\alpha_i}_{v_f j_f v_i j_i}D^{\alpha_f\alpha_i}_{v_f j_f v_i j_i}(E)\,. \tag{28}$$

A. Bound-to-bound transitions

The cross section of interest is obtained by averaging Eq. (28) over a Boltzmann distribution of initial rotational states characterized by a rotational temperature $T_{\rm rot}$ and summing over all final vibrational and rotational states:

$$\sigma^{\alpha_i\alpha_f}_{v_i}(E,T_{\rm rot})=[Q^{\alpha_i}_{v_i}(T_{\rm rot})]^{-1}\left[\sum_{j_i=0}^{j_i^{\max}}d_{j_i}(2j_i+1)\exp(-\varepsilon^{\alpha_i}_{v_i j_i}/k_BT_{\rm rot})\sum_{v_f=0}^{v_f^{\max}}\sum_{j_f}\sigma^{\alpha_i\alpha_f}_{v_i j_i v_f j_f}(E)\right]\,, \tag{29}$$

where $Q^{\alpha_i}_{v_i}(T_{\rm rot})$ is the rotational partition function for vibronic state (α_i,v_i),

$$Q^{\alpha_i}_{v_i}(T_{\rm rot})=\sum_{j_i=0}^{j_i^{\max}}d_{j_i}(2j_i+1)\exp(-\varepsilon^{\alpha_i}_{v_i j_i}/k_BT_{\rm rot})\,, \tag{30}$$

k_B is Boltzmann's constant, and $v_f^{\max}$ is the vibrational quantum number of the highest bound state of the final electronic state. The nuclear-spin degeneracy factor d_{j_i} is unity except for certain classes of homonuclear diatomics (see Table I). $j_i^{\max}$ is selected by practical consideration.

The sum over final rotational states has nonzero contributions only for j_f equal to j_i-1 or j_i+1 ($j_f\geqq0$). In the low-temperature limit, only the $j_i=0$ and $j_f=1$ states contribute to $\sigma^{\alpha_i\alpha_f}_{v_i}(E,T_{\rm rot})$. Then the sums over the Clebsch-Gordan coefficients in Eq. (19) can be evaluated to give a factor of $\frac{1}{9}$ and the cross section of Eq. (29) reduces to

TABLE I. Nuclear-spin degeneracy factors required for homonuclear diatomic molecules in sigma states.

	d_j	
	g^+ or u^- and $2I+1$ even, or g^- or u^+ and $2I+1$ odd	g^- or u^+ and $2I+1$ even, or g^+ or u^- and $2I+1$ odd
Even j	$(I+1)(2I+1)$	$I(2I+1)$
Odd j	$I(2I+1)$	$(I+1)(2I+1)$

$$\sigma_{v_i}^{\alpha_i\alpha_f}(E,T_{\rm rot})\rightarrow\sum_{v_f=0}^{v_f^{\max}}\frac{m_e^2e^2}{3\hbar^4}(2-\delta_{\Lambda_f,0})(M_{v_fv_i}^{\alpha_f\alpha_i})^2D_{v_fv_i}^{\alpha_f\alpha_i}\quad\text{as } T_{\rm rot}\rightarrow 0\ . \tag{31}$$

Invoking the Franck-Condon approximation in Eq. (12) and assuming the vibrational states are degenerate we obtain[30]

$$\sigma_{if}(E,T_{\rm rot})\rightarrow\frac{m_e^2e^2}{3\hbar^4}(2-\delta_{\Lambda_f,0})[M_{\alpha_f\alpha_i}(R_{\rm eq})]^2D^{\alpha_f\alpha_i}(E)\quad\text{as } T_{\rm rot}\rightarrow 0\ , \tag{32}$$

where we assume the sum over the Franck-Condon factors is unity (this is true only if continuum states are also included in the "sum"). This expression thus represents excitation to both bound and dissociative states. We call the cross section denoted by Eq. (29) the IPVR (impact-parameter-method, vibrational-rotational) cross section, the one given by Eq. (31) the IPV (impact-parameter-method, vibrational) cross section, and the one given by Eq. (32) the IP (impact-parameter-method) cross section. The last is the form obtained by Hazi.[30]

B. Bound-to-continuum transitions

Next we consider the modification necessary for dissociative transitions. In this case we no longer have a vibrational quantum number for the final state; instead we have the continuum energy ε. Thus we replace all occurrences of the quantum number v_f by ε in the preceding equations. The wave functions for the continuum states are solutions to the equation

$$[-(\hbar^2/2\mu_{AB})d^2/dR^2+V_{\alpha_f}(R)+\hbar^2l_f(l_f+1)/2\mu_{AB}R^2]\chi_{\varepsilon l_f}^{\alpha_f}(R)=\varepsilon\chi_{\varepsilon l_f}^{\alpha_f}(R) \tag{33}$$

subject to scattering boundary conditions, i.e.,

$$\chi_{\varepsilon l_f}^{\alpha_f}(R)\rightarrow 0\ \text{ as } R\rightarrow 0\ , \tag{34}$$

$$\chi_{\varepsilon l_f}^{\alpha_f}(R)\rightarrow CkR[j_{l_f}(kR)-\tan(\eta)n_{l_f}(kR)]\ \text{ as } R\rightarrow\infty\ , \tag{35}$$

where

$$k=(2\mu_{AB}/\hbar)[\varepsilon-V_{\alpha_f}(R=\infty)]\ , \tag{36}$$

j_{l_f} and n_{l_f} are regular and irregular Riccati-Bessel functions,[40] respectively, η is the phase shift, and C is a constant obtained by normalizing the wave function to unit density per unit energy.[12] The transition energy ΔE [Eq. (27)] is replaced by

$$\Delta E=\varepsilon-\varepsilon_{v_ij_i}^{\alpha_i} \tag{37}$$

and the final expression for the averaged cross section is

$$\sigma_{v_i}^{\alpha_i\alpha_f}(E,T_{\rm rot})=[Q_{v_i}^{\alpha_i}(T_{\rm rot})]^{-1}\left[\sum_{j_i=0}^{j_i^{\max}}d_{j_i}(2j_i+1)\exp(-\varepsilon_{v_ij_i}^{\alpha_i}/k_BT_{\rm rot})\sum_{l_f}\int_{\varepsilon_{\min}}^{\varepsilon_{\max}}d\varepsilon\,\sigma_{v_ij_i\varepsilon l_f}^{\alpha_i\alpha_f}(E)\right]\ , \tag{38}$$

where, in analogy to Eq. (28),

$$\sigma_{v_ij_i\varepsilon l_f}^{\alpha_i\alpha_f}(E)=S_{\varepsilon l_fv_ij_i}^{\alpha_f\alpha_i}D_{\varepsilon l_fv_ij_i}^{\alpha_f\alpha_i}(E)\ . \tag{39}$$

In this case, the final rotational angular momentum quantum number is interpreted as the orbital angular momentum quantum number l_f of the separating atoms. We refer to the cross section defined by Eq. (38) as the IPVRD (impact-parameter-method, vibrational-rotational dissociation) cross section. The limits of integration in Eq. (38) are rigorously given by the continuum threshold

$$\varepsilon_{\min}=V_{\alpha_f}(R=\infty) \tag{40}$$

and by energy conservation

$$\varepsilon_{\max}=E+\varepsilon_{v_ij_i}^{\alpha_i}\ . \tag{41}$$

The expression for dissociation from selected initial vibrational states in which rotations are treated as degenerate is generalized from Eq. (31),

$$\sigma_{v_i}^{\alpha_i\alpha_f}(E)=\int_{\varepsilon_{\min}}^{\varepsilon_{\max}}d\varepsilon\,D_{\varepsilon v_i}^{\alpha_f\alpha_i}(E)S_{\varepsilon v_i}^{\alpha_f\alpha_i}\ , \tag{42}$$

where the structural factor is given by

$$S_{\varepsilon v_i}^{\alpha_f\alpha_i}=\frac{m^2e^2}{3\hbar^4}(2-\delta_{\Lambda_f,0})\,|\,M_{\varepsilon v_i}^{\alpha_f\alpha_i}\,|^2 \tag{43}$$

and the dynamical factor is given by Eqs. (21)—(26). The cross section defined by Eq. (42) is called the IPVD

(impact-parameter-method, vibrational dissociation) cross section.

III. COMPUTATIONAL DETAILS

The potential curves for the $X\,^1\Sigma_g^+$, $B\,^1\Sigma_u^+$, and $B'\,^1\Sigma_u^+$ states of H_2 are obtained by fitting accurate *ab initio*[41,42] and experimental[43] data in a manner similar to that of Blais and Truhlar.[44] Over the region for which the potential data is available, the points are fitted to a cubic spline function. For small R values the potential is written as

$$V = AR^{-1}\exp(-BR)\,, \tag{44}$$

where the parameters A and B are determined so that the function fits the data points at the two smallest R values. For the region of R values greater than the spline-fit region, the potential is fitted with the form

$$V = V_0 - C_6R^{-6} - C_8R^{-8}\,, \tag{45}$$

where V_0 is the experimental dissociation energy and the parameters C_6 and C_8 are determined so that the function fits the data points at the two largest R values. The cubic spline fit is restricted to match the function values and their derivatives at the end points of the data. Our fits to the three potential curves used in this work are presented in Fig. 1.

The transition dipole matrix elements as a continuous function of R are obtained by 4-point (third-order) Lagrange interpolation[40] of the accurate *ab initio* data.[45,46] The fits to the matrix elements are shown in Fig. 2.

The vibrational eigenvalues $\varepsilon_{vj}^{\alpha}$ are obtained by solving Eq. (3) using Cooley's algorithm.[47] Once an eigenvalue is found, the values of the unnormalized wave function $\chi_{vj}^{\alpha}(R)$ are stored on a grid of evenly spaced R values.

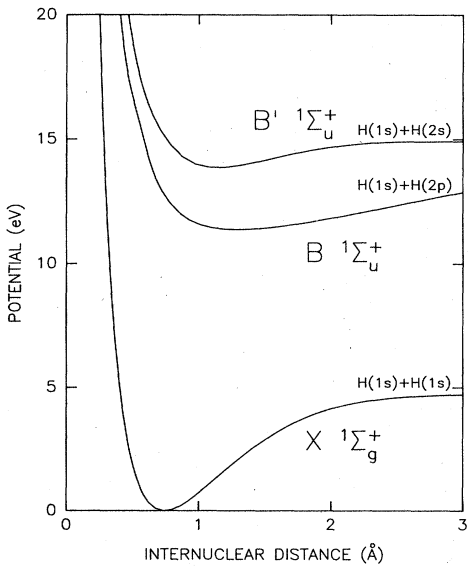

FIG. 1. Potential-energy curves for the three states of H_2 studied in this work. The $X\,^1\Sigma_g^+$ and $B\,^1\Sigma_u^+$ potentials are fits to the calculations of Kolos and Wolniewicz (Refs. 41 and 42, respectively), while the $B'\,^1\Sigma_u^+$ potential is a fit to the data of Spindler (Ref. 43).

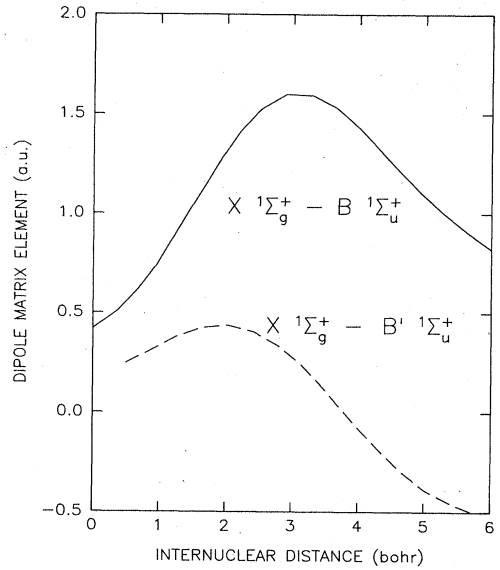

FIG. 2. Dipole matrix elements used in the calculations. The matrix element for the $X\,^1\Sigma_g^+$ to $B\,^1\Sigma_u^+$ transition is a fit to the calculation of Wolniewicz (Ref. 45) while that for the $X\,^1\Sigma_g^+$ to $B'\,^1\Sigma_u^+$ transition is a fit to the calculation of Ford (Ref. 46).

The normalization factor is determined by extended Simpson's-rule integration,[40] and the stored values are normalized. Unnormalized continuum wave functions for a fixed energy ε are obtained by Numerov integration and stored on the same grid of R values used for the vibrational wave function. The asymptotic boundary conditions are applied, and the normalization constant of Eq. (35) is obtained using the method described by Chung, Lin, and Lee.[12]

The structural factor $S_{v_fj_fv_ij_i}^{\alpha_f\alpha_i}$ is obtained from Eq. (19), where the summation over the Clebsch-Gordan coefficients is straightforward and the square of the dipole transition matrix element is obtained from Eq. (12). The integration in Eq. (12) is performed using extended Simpson's rule on the grid of R values on which the wave functions are saved. In the case of bound-to-continuum transitions, the quantum number v_f is replaced by the energy eigenvalue ε, but the computational procedure is identical.

The dynamical factor is calculated from Eq. (21). Evaluation of all of the modified Bessel and Struve functions, including the finite integral of the Struve function, is accomplished by Lagrange interpolation from the tables of Abramowitz and Stegun.[40] The order of interpolation used is that recommended in the tables.

The impact-parameter method requires that a minimum value of the orbital angular momentum of the incident electron be supplied to evaluate Eq. (21). For the comparisons reported here, we have used Hazi's value ($b_0 = 1.7a_0$).[30] In subsequent applications, we define the minimum value of the impact parameter b_0 by requiring the cross section from Eq. (32) to agree with that of the Born approximation at a high energy.[30] The choice of b_0 is discussed further in paper II.[48]

For dissociative processes, the integral over the final energy is performed using repeated Gauss-Legendre integration. The total range from ε_{min} to ε_{max} need not be considered; only a limited range of ε values contributes significantly to the cross sections for all incident energies. This range is determined by the behavior of the Franck-Condon factors. Typically 80 to 100 integration points are needed to converge the cross sections to two or more significant figures.

IV. RESULTS

In this section we report the results of calculations of various electron-impact processes in H_2 using the theoretical impact-parameter methods of Sec. II. The calculations permit comparison with experimental and other theoretical results. We have studied excitation and dissociation of ground-state H_2 via the B and B' states and the effect of varying initial molecular vibrational and rotational energy on these processes. The latter studies are the first of their kind for electron-impact dissociation to neutral species.

In Table II we present cross sections for electron-impact excitation from the ground (X) state to the B state of H_2 ($v=0$). Our IPV results [Eq. (31)] are compared with other theoretical calculations and with experiment. The comparison is also shown in Fig. 3. Because the level of theory in our IPV calculations [Eq. (31)] is meant to be comparable to the treatment of vibration in the majority of other theoretical methods, we use the Franck-Condon approximation in Eq. (12) for the comparisons in Table II. Our most accurate method employs explicit numerical integration of the dipole transition moment over the vibrational wave functions of the target molecule.

The agreement of the Born-approximation results[16,23] with our IPV cross sections in Table II is good at energies above 50 eV but poorer at lower energies, where the Born approximation is known to break down. The fact that the two sets of Born-approximation results appear to have a different low-energy behavior is somewhat disturbing. The difference is larger between the two Born cross sections than that found in comparing the smaller Born cross section with the Born-Ochkur result[16] (which included exchange). Fliflet and McCoy[23] attribute this difference to the use of different final-state wave functions. The IPV results are in reasonable agreement with the distorted-

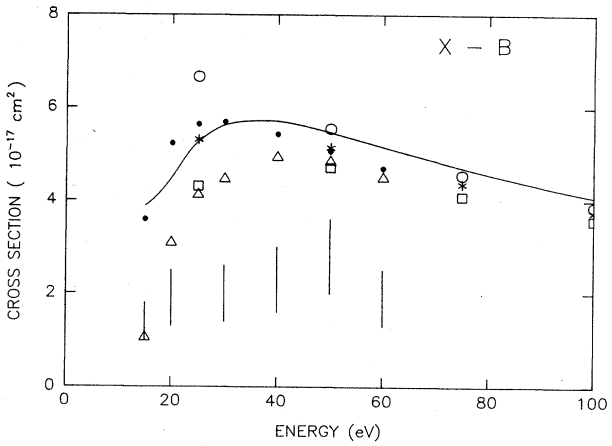

FIG. 3. Electron-impact excitation cross sections (units of 10^{-17} cm^2) for the $X\,^1\Sigma_g^+$ ($v=0$) to $B\,^1\Sigma_u^+$ transition in H_2. The solid curve represents the results (summed over final vibrational states) of the present impact-parameter IPV cross section [Eq. (31)] with the Franck-Condon approximation used to evaluate the vibrational integrals in Eq. (12). The circles and solid circles are the results of Born approximation calculations (Refs. 16 and 23, respectively). The triangles are from the L^2 distorted-wave calculations of Ref. 23. The asterisks are the Born-Ochkur calculations of Ref. 16, and the squares are the results of two-state close-coupling calculations. The vertical lines represent error bars for the experimental results of Ref. 32.

TABLE II. Comparison of the present impact-parameter results for the electron-impact excitation of the B state of H_2 with other results.[a]

E (eV)	CC[b]	Born I[c]	BO[d]	DW[e]	Born II[f]	IPV[g]	Expt.[h]
15				1.05	3.60	3.61	1.4±0.4
20				3.09	5.23	4.10	1.9±0.6
25	4.31	6.66	5.31	4.12	5.64	4.84	
30				4.46	5.69	5.19	2.0±0.6
40				4.93	5.43	5.27	2.3±0.7
50	4.71	5.55	5.14	4.84	5.06	5.06	2.8±0.8
60				4.49	4.70	4.79	1.9±0.6
75	4.09	4.55	4.36			4.37	
100	3.58	3.87	3.76			3.80	

[a]Cross sections are in units of 10^{-17} cm^2. Results are for 0 K.
[b]Two-state close-coupling results of Ref. 16.
[c]Born results of Ref. 16.
[d]Born-Ochkur results of Ref. 16.
[e]L^2 distorted-wave results of Ref. 23.
[f]Born results of Ref. 23.
[g]IPV results of the present work from Eq. (31) with the Franck-Condon evaluation of vibrational integrals.
[h]Experimental data from Ref. 32.

wave (Ref. 23) cross sections, being somewhat larger at the lower energies. The close-coupling results[16] are also smaller than the IPV cross sections, but the overall agreement of the present impact-parameter method with both of these more exact methods is within an acceptable 15% above 25 eV. The distorted-wave[23] and close-coupling[16] calculations include exchange, which is not treated in the impact-parameter theory. Exchange effects could be included in the IP method by the use of effective exchange potentials.[49] However, one should then account for higher-order terms in the expansion Eq. (6).

The experimental results of Srivastava and Jensen[32] lie about a factor of 2 below all of the theoretical calculations. Their experiment did not directly measure the integrated cross section to all final vibrational states; it only detected radiation from the $v'=2$ state. The quantity they measured was the differential cross section, which agreed well with the distorted- wave calculations of Fliflet and McCoy[23] except in the low-angle region, where the experimental cross section was about a factor of 2 smaller than the calculations. The cross section summed over all final vibrational states was estimated using the Franck-Condon principle. The differences between the theoretical and experimental cross sections in Table II probably stem from the smaller values for low-angle scattering obtained in the experiment. The good agreement above threshold among all of the theoretical methods suggests that the predicted values of the excitation cross sections in this energy region for the X-to-B transition in H_2 are reliable.

In Table III we compare the results for this transition of various treatments of molecular vibration within the impact-parameter method. The IP (impact-parameter) method of Hazi,[30] which assumes vibrational degeneracy, underestimates the IPV cross sections obtained with an accurate treatment of vibration (shown in the rightmost column) by approximately 10%. The use of IPV with the

TABLE III. Comparison of various impact-parameter approximations for the X to B excitation of H_2.[a]

E (eV)	IP[b]	IPV(FC)[c]	IPV[d]
15	3.47	3.61	3.87
20	3.83	4.10	4.47
25	4.58	4.84	5.25
30	4.95	5.19	5.61
35	5.09	5.29	5.72
40	5.08	5.27	5.68
45	5.01	5.18	5.58
50	4.90	5.06	5.45
55	4.78	4.93	5.30
60	4.64	4.79	5.14
70	4.39	4.51	4.84
75	4.26	4.37	4.69
80	4.14	4.25	4.57
85	4.02	4.12	4.42
90	3.91	4.01	4.30
95	3.81	3.90	4.18
100	3.71	3.80	4.07

[a]Cross sections are in units of 10^{-17} cm^2. Results are for 0 K.
[b]IP results [Eq. (32)] corresponding to Hazi's method of Ref. 30. Continuum contributions (small in this case) are implicitly included.
[c]IPV results [Eq. (31)], with the Franck-Condon approximation used to evaluate integrals over the vibrational wave functions.
[d]IPV results [Eq. (31)], with the integrals over vibrational wave functions evaluated explicitly.

TABLE IV. Cross sections for electron-impact excitation from the X to the B' state of H_2.[a]

E (eV)	Born[b]	DW[c]	IP[d]	IPV(FC)[e]	IPV[f]
20	8.88	1.7	4.03	1.93	2.14
30		3.9	5.49	2.66	2.95
40		4.8	6.19	2.89	3.21
50	9.41	4.9	6.28	2.88	3.19
60		4.7	6.14	2.78	3.08
70		4.4	5.91	2.66	2.94
80		4.1	5.79	2.53	2.80
90		3.8	5.42	2.41	2.67
100	6.75	3.4	5.18	2.30	2.54

[a]Cross sections are in units of 10^{-18} cm^2. Results are for 0 K.
[b]Born results of Ref. 15.
[c]L^2 distorted-wave results interpolated from Fig. 4 of Ref. 26.
[d]Impact-parameter IP results from Eq. (32) corresponding to the original method of Hazi [Ref. 30] which assumes vibrational degeneracy. Continuum contributions, implicit in this method, are large for this case.
[e]Impact-parameter results with the IPV cross section of Eq. (31). The vibrational integrals are evaluated using the Franck-Condon approximation.
[f]Impact-parameter results with the IPV cross section of Eq. (31). The vibrational integrals are evaluated using numerical integration.

TABLE V. Electron-impact dissociation cross sections for production of $H(1s)+H(2s)$ via excitation to the B' state of H_2.[a]

E (eV)	BR[b]	DW[c]	IPVD(FC)[d]	IPVD[e]	Expt.[f]
20	1.98	1.48	2.32	2.24	
30		3.23	3.12	3.02	
40	3.91	4.46	3.54	3.41	
50			3.60	3.47	6.17
60	3.75	4.41	3.52	3.40	5.94
70			3.40	3.28	
80	3.41		3.26	3.14	5.50
90			3.12	3.00	
100	3.09	3.41	2.99	2.88	5.08
150	2.50		2.44	2.35	4.19
200	2.10		2.07	1.99	3.62
250			1.80	1.73	3.10
300			1.60	1.54	2.69

[a]Cross sections are in units of 10^{-18} cm^2. Results are for 0 K.
[b]Born-Rudge results of Ref. 12.
[c]L^2 distorted-wave results of Ref. 26.
[d]Impact-parameter results with IPVD cross section from Eq. (42) evaluated using the Franck-Condon approximation for vibrational integrals.
[e]Impact-parameter results with IPVD cross section from Eq. (42) with the vibrational integrals evaluated numerically.
[f]Experimental results of Ref. 33 scaled by 0.8 according to the recommendation of Ref. 34. The experimental cross section contains contributions from states other than B'.

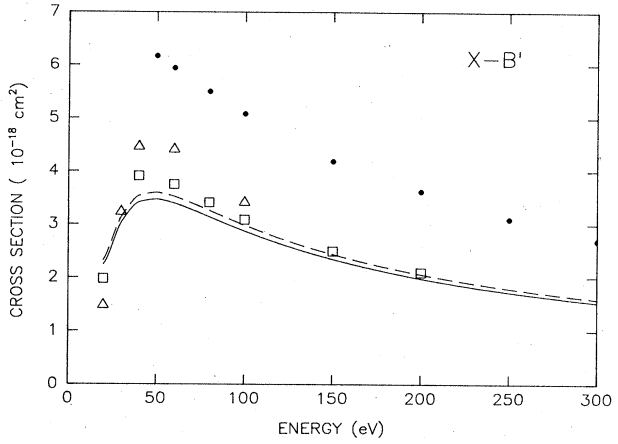

FIG. 4. Electron-impact dissociation cross sections (in units of 10^{-18} cm^2) for production of H(1s)+H(2s) via excitation of the $B'\,^1\Sigma_u^+$ ($v=0$) state of H_2. The solid curve is the result of applying the IPVD method [Eq. (42)] of Sec. II B with accurate numerical evaluation of the integrals over vibrational wave functions. The dashed curve represents the IPVD result when the Franck-Condon approximation is used to evaluate the integrals [Eq. (12)] . The squares represent the Born-Rudge results of Ref. 12 and the triangles represent the L^2 distorted-wave results of Ref. 26. The experimental results of Ref. 33 (multiplied by 0.8 according to the recommendation of Ref. 34) are shown as solid circles. The experimental results include contributions from states other than $B'\,^1\Sigma_u^+$.

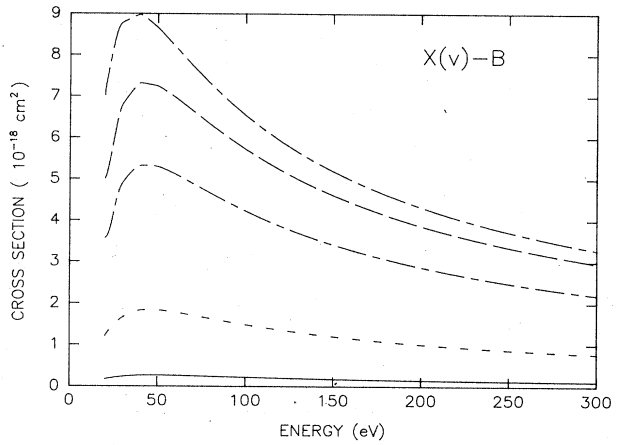

FIG. 6. Dependence on initial vibrational quantum number of the electron-impact dissociation cross section to produce H(1s)+H(2p) via the $B\,^1\Sigma_u^+$ state of H_2 (in units of 10^{-18} cm^2). The solid curve represents $v=0$, the dashed curve $v=1$, the long-dash—short-dash curve $v=2$, the long-dash curve $v=5$, and the long-dash—double-short-dash curve $v=10$.

Franck-Condon (FC) approximation in Eq. (12) shows the improvement over IP [Eq. (32)] that can be achieved by including vibrational motion. The IP method (Ref. 30) implicitly assumes a sum over bound and continuum vibrational levels, while the IPV method only includes bound levels. For this comparison, however, the major differences arise from errors in treating these bound states since the dissociation cross section is small. This comment applies only for this case ($v=0$). As will be seen below, there is a considerable enhancement of the dissociation cross section with increasing target vibrational excitation.

Table IV presents results from excitation to the B' state of H_2. For this transition there are fewer calculations for comparison and (to our knowledge) no experimental results. The most accurate theoretical calculations available for comparison are the distorted-wave results of Mu-Tao, Lucchese, and McCoy.[26] These results include bound vibrational states through a Franck-Condon factor in the differential cross section so that the most meaningful comparison is with our IPV(FC) calculations in the fourth column. The agreement with the present IPV cross sec-

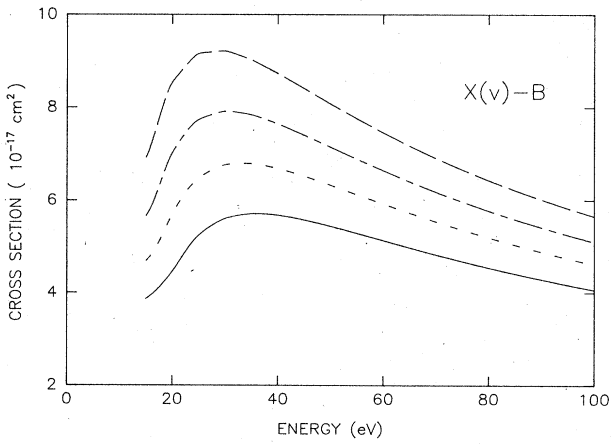

FIG. 5. Dependence of the cross section (summed over final vibrational states) for excitation of the $B\,^1\Sigma_u^+$ state on initial vibrational quantum number (in units of 10^{-17} cm^2). The solid curve represents $v=0$, the dashed curve $v=1$, the long-dash—short-dash curve $v=2$, and the long-dash curve $v=3$.

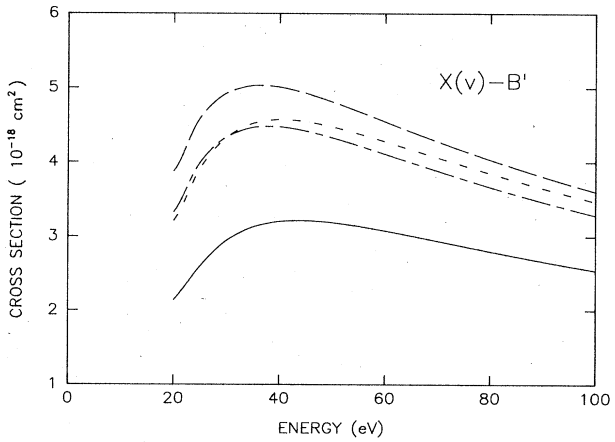

FIG. 7. Dependence of the cross section (summed over final vibrational states) for excitation of the $B'\,^1\Sigma_u^+$ state on initial vibrational quantum number (in units of 10^{-18} cm^2). The solid line represents $v=0$, the dashed line $v=1$, the long-dash—short-dash curve $v=2$, as the long-dash curve $v=3$.

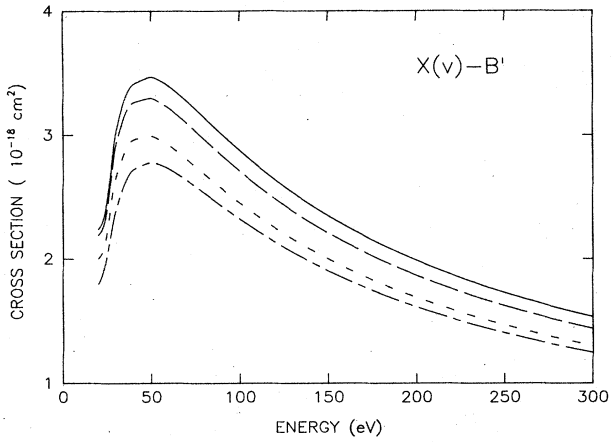

FIG. 8. Dependence on initial vibrational quantum number of the electron-impact dissociation cross section to produce $H(1s)+H(2s)$ via the $B'\,^1\Sigma_u^+$ state of H_2 (in units of 10^{-18} cm^2). The solid curve represents $v=0$, the long-dash—short-dash curve $v=1$, the long-dash curve $v=2$, and the short-dash curve $v=3$.

tions [Eq. (31)] is typically to within 30% to 40% of the distorted-wave (Ref. 26) result. The agreement between the present results and the Born-approximation calculations of Arrighini *et al.*[15] is poor, the difference being a factor of 4 at low energies. The simple IP method [Eq. (32)] overestimates the IPV and DW (Ref. 23) cross sections by approximately a factor of 2. This is due to the implicit sum over continuum states discussed above for the IP method [Eq. (32)]. The sum over all bound vibrational levels of the B' state of the Franck-Condon factors involving ground-state H_2 is 0.48, so that approximately 50% of the IP cross section comes from the continuum. This comparison of the IP and IPV cross sections indicates that a realistic treatment of molecular vibration is important for this transition due to the importance of dissociative processes.

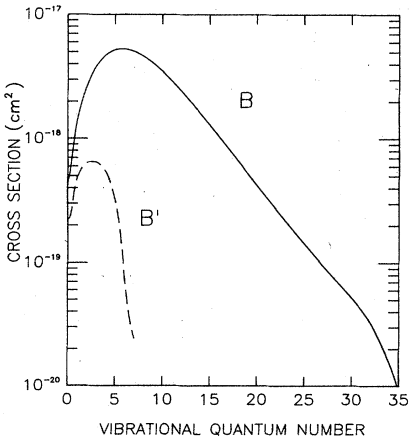

FIG. 9. Final vibrational distributions (in units of cm^2) of the $B\,^1\Sigma_u^+$ and $B'\,^1\Sigma_u^+$ states of H_2 resulting from electron-impact excitation of the $X\,^1\Sigma_u^+$ ($v=0$) state.

In Table V we present cross sections for the production of $H(1s)+H(2s)$ via excitation to continuum levels of the B' state. The agreement between the various theoretical results is good; the largest difference is less than 20% at energies above the maximum in the cross section. The theoretical results all lie approximately 50% below the experimental results of Vroom and de Heer[33]. The latter have been scaled by 0.8 as suggested by Mumma and Zipf[34] to correct for molecular radiation observed in the experiment. Because the experimental cross sections contain contributions from other states that produce $H(1s)+H(2s)$, they are expected to be larger than the theoretical calculations. Figure 4 illustrates these results and shows the good agreement of the various theoretical treatments.

In Fig. 5 the effect of increasing the energy in molecular vibration (up to $v=3$) for the bound-bound X-B transition is shown. For this range of vibrational quanta the cross section doubles. In Fig. 6 the corresponding vibrational dependence for dissociative excitation is seen to be even greater, although the cross sections are smaller than for nondissociative excitation. The enhancement in both cases results form the larger Franck-Condon factors for the excited vibrational levels of the X state.

In Fig. 7 the vibrational dependence of the cross section for nondissociative X-B' excitation is shown. Instead of increasing monotonically with v, the $v=1$ and $v=2$ cross sections reverse order. The cross sections for dissociation to $H(1s)+H(2s)$ in Fig. 8 are monotonically decreasing with v, in contrast to all of the other processes discussed here. Again, this behavior is primarily determined by the magnitude of the structural factor.

The impact-parameter method as formulated in this work is capable of providing information on final-state vibrational distributions. In Fig. 9 we show vibrational distributions for both the B and B' states resulting from electron-impact excitation from the ground vibrational level of the X state. The two distributions reflect the difference in the number of vibrational levels supported by the two excited electronic states. Both the B and B' distributions have maxima for $v>0$, indicating a preference for vibrationally inelastic processes.

Table VI presents the rotational-temperature depen-

TABLE VI. Rotational-temperature dependence of the cross section for electronic excitation to the B state of H_2.[a]

	Temperature (kelvin)					
E (ev)	0	4.2	300	1000	5000	20 000
15	3.87	3.87	3.89	3.94	4.31	5.53
20	4.47	4.46	4.49	4.57	5.15	6.83
25	5.25	5.24	5.27	5.37	5.97	7.63
30	5.61	5.60	5.63	5.72	6.31	7.93
35	5.72	5.70	5.74	5.82	6.39	7.91
40	5.68	5.67	5.71	5.79	6.32	7.75
45	5.58	5.57	5.60	5.68	6.19	7.54
50	5.45	5.44	5.47	5.54	6.02	7.29
60	5.14	5.14	5.15	5.23	5.66	6.81
80	4.55	4.55	4.57	4.63	5.00	5.95
100	4.07	4.06	4.08	4.14	4.45	5.27

[a]Cross sections from Eq. (29) are in units of 10^{-17} cm^2.

TABLE VII. Rotational-temperature dependence of the cross section for electronic excitation to the B' state of H_2.[a]

	Temperature (kelvin)					
E (eV)	0	4.2	300	1000	5000	20000
20	2.10	2.10	2.10	2.14	1.87	1.65
30	2.90	2.90	2.89	2.94	2.57	2.27
40	3.15	3.15	3.14	3.19	2.78	2.44
50	3.13	3.13	3.12	3.17	2.75	2.42
60	3.03	3.03	3.01	3.06	2.65	2.32
80	2.82	2.82	2.74	2.78	2.41	2.12
100	2.50	2.50	2.49	2.52	2.18	1.92

[a]Cross sections from Eq. (29) are in units of 10^{-18} cm^2.

TABLE VIII. Rotational-temperature dependence of the cross section for dissociation of H_2 through the B' state.[a]

	Temperature (kelvin)					
E (eV)	0	4.2	300	1000	5000	20000
20	2.28	2.28	2.31	2.40	2.77	2.96
30	3.06	3.06	3.11	3.24	3.77	4.04
40	3.46	3.46	3.51	3.65	4.21	4.49
50	3.52	3.52	3.57	3.70	4.25	4.53
60	3.45	3.45	3.49	3.62	4.14	4.41
80	3.19	3.19	3.23	3.34	3.81	4.05
100	2.92	2.92	2.96	3.06	3.48	3.69
150	2.38	2.38	2.42	2.50	2.84	3.00
200	2.02	2.02	2.04	2.12	2.40	2.54
250	1.76	1.76	1.78	1.84	2.08	2.20
300	1.56	1.56	1.58	1.63	1.85	1.95

[a]Cross sections are in units of 10^{-18} cm^2.

dence of the X-B excitation of H_2 initially in the ground vibrational state. The cross section increases by approximately 45% over the temperature range from zero to 20000 K. The corresponding dissociative cross section (not shown) to form $H(1s)+H(2p)$ increases by 30% over the same range of temperatures. For $v=0$ the dissociation cross section has a maximum for 300 K of 2.9×10^{-19} cm^2 at 50 eV compared to 5.6×10^{-17} cm^2 for the bound-bound excitation. For the X-B transition bound-bound transitions dominate over bound-continuum processes regardless of rotational temperature or initial vibrational temperature. The effect of initial vibrational energy is much more significant than the effect of rotational temperature.

In Table VII the nondissociative excitation cross section for the X-B' transition decreases monotonically with temperature. This is the opposite of the behavior seen in Table VI for the X-B transition. The explanation lies in the far-fewer bound rotational states that can be supported by the B' electronic state. At higher temperatures, therefore, the tail of the Boltzmann distribution becomes severely truncated. The cross sections for dissociation through the B state, shown in Table VIII, increase monotonically with temperature. We also found this increase with temperature for the X-B dissociation cross sections. We are not reporting the latter since they are small in magnitude for $v=0$ (the only case studied when rotational motion was included) and the trends follow those for the B' state.

V. CONCLUSIONS

The purpose of this work was to extend the impact-parameter method for diatomic molecules to permit a realistic treatment of vibrational and rotational motion and to allow the study of dissociative processes. To test the theory, applications were made to nondissociative excitation of the B state of H_2 and to dissociation to $H(1s)+H(2s)$ via the B' state. Agreement with previous theoretical results is generally good. Comparison with experiment was hampered by the lack of direct experimental information for the processes we studied. However, the magnitudes of the theoretical cross sections are very consistent with our understanding of the processes probed by the experiments. New results from this work include the dependence on initial vibrational state and rotational temperature of nondissociative and dissociative processes involving the X, B, and B' states of H_2. While the dependence of the cross sections on initial rotational temperature is modest, we find that increasing initial vibrational energy can have a dramatic effect on the cross sections. There is to our knowledge no experimental data providing information on the effect of internal energy on the processes reported here. However, the trends we find concerning the effect of internal energy on dissociation are similar to those seen in dissociative attachment processes in H_2.[50,51]

In summary, the impact-parameter theory presented here should be useful in studying the effect of internal energy in excitation and dissociation processes in diatomic molecules. It is a first-order theory, and thus is most valid at high energies, i.e., at some distance above threshold. It is also best applied to qualitative studies of integral cross sections. Applications of the methods developed here to heavier diatomic molecules are given in paper II (Ref. 8) and in forthcoming publications.[52,53]

ACKNOWLEDGMENTS

This research was supported by the Air Force Wright Aeronautical Laboratories, Aero Propulsion Laboratory, Air Force Systems Command, U. S. Air Force, Wright-Patterson Air Force Base, Ohio 43433 under Contract No. F33615-82-C-2241. The authors thank Dr. Andrew Hazi for helpful discussions.

*Permanent address: Department of Chemistry, Ohio State University, Columbus, OH 43210.

[1]G. J. Schultz, in *Principles of Laser Plasmas,* edited by B. Bekefi (Wiley, New York, 1976), p. 33.

[2]See, for example, *Abstracts of the Thirteenth International Conference on the Physics of Electronic and Atomic Collisions, Berlin, 1983,* edited by J. Eichler, W. Fritsch, I. V. Hertel, N. Stolterfoht, U. Wille (North-Holland, Amsterdam, 1983); S. Trajmar and D. C. Cartwright, in *Electron-Molecule Interactions and Their Applications,* Vol. I, edited by L. G. Christo-

phorou (Academic, New York, 1984), p. 155.
[3]*Electron-Molecule and Photon-Molecule Collisions,* edited by T. Rescigno, V. McKoy, and B. Schneider (Plenum, New York, 1979).
[4]N. F. Lane, Rev. Mod. Phys. **52**, 29 (1980).
[5]*Electron-Atom and Electron-Molecule Collisions,* edited by J. Hinze (Plenum, New York, 1983).
[6]S. P. Khare and B. L. Moiseiwitsch, Proc. Phys. Soc. London **88**, 605 (1966).
[7]S. P. Khare, Phys. Rev. **157**, 107 (1967).
[8]K. J. Miller and M. Krauss, J. Chem. Phys. **47**, 3754 (1967).
[9]M. Inokuti, Rev. Mod. Phys. **43**, 297 (1971).
[10]D. C. Cartwright, Phys. Rev. A **2**, 1331 (1970); **5**, 1974 (1972).
[11]S. Chung and C. C. Lin, Phys. Rev. A **6**, 988 (1972); **9**, 1954 (1974).
[12]S. Chung, C. C. Lin, and E. T. P. Lee, Phys. Rev. A **12**, 1340 (1975).
[13]C. W. McCurdy and V. McKoy, J. Chem. Phys. **61**, 2820 (1974).
[14]T. N. Rescigno, C. F. Bender, and V. McKoy, J. Phys. B **8**, L433 (1975).
[15]G. P. Arrighini, F. Biondi, C. Guidotti, A. Biagi, and F. Marinelli, Chem. Phys. **52**, 133 (1980).
[16]S. Chung and C. C. Lin, Phys. Rev. A **17**, 1874 (1978).
[17]C. A. Weatherford, Phys. Rev. A **22**, 2519 (1980).
[18]T. K. Holly, S. Chung, C. C. Lin, and E. T. P. Lee, Phys. Rev. A **26**, 1852 (1982).
[19]T. K. Holly, S. Chung, C. C. Lin, and E. T. P. Lee, Phys. Rev. A **24**, 2946 (1981).
[20]T. N. Rescigno, C. W. McCurdy, V. McKoy, and C. F. Bender, J. Phys. B **8**, 216 (1976).
[21]T. N. Rescigno, C. W. McCurdy, V. McKoy, and C. F. Bender, Phys. Rev. A **13**, 216 (1976).
[22]A. W. Fliflet, Ref. 1, p. 87.
[23]A. W. Fliflet and V. McKoy, Phys. Rev. A **21**, 1863 (1980).
[24]A. W. Fliflet, V. McKoy, and T. N. Rescigno, J. Phys. B **12**, 3281 (1979).
[25]A. W. Fliflet, V. McKoy, and T. N. Rescigno, Phys. Rev. A **21**, 788 (1980).
[26]Lee Mu-Tao, R. R. Lucchese, and V. McKoy, Phys. Rev. A **26**, 3240 (1982).
[27]B. D. Buckley and P. G. Burke, Ref. 1, p. 133.
[28]M. J. Seaton, Proc. Phys. Soc. London **79**, 1105 (1962).
[29]A. D. Stauffer and M. R. C. McDowell, Proc. Phys. Soc. London **85**, 61, (1965); **89**, 289 (1966).
[30]A. W. Hazi, Phys. Rev. A **23**, 2232 (1981).
[31]A. W. Hazi, T. N. Rescigno, and A. E. Orel, Appl. Phys. Lett. **35**, 477 (1979).
[32]S. K. Srivastava and S. Jensen, J. Phys. B **10**, 3341 (1978).
[33]D. A. Vroom and F. J. de Heer, J. Chem. Phys. **50**, 580 (1969).
[34]M. J. Mumma and E. C. Zipf, J. Phys. Chem. **55**, 1661 (1971).
[35]M. Shugard and A. Hazi, Phys. Rev. A **12**, 1895 (1975).
[36]G. Herzberg, *Molecular Spectra and Molecular Structure* (Van Nostrand, New York, 1950).
[37]D. M. Brink and G. R. Satchler, *Angular Momentum* (Clarendon, Oxford, 1968).
[38]G. Arfken, *Mathematical Methods for Physicists* (Academic, New York, 1968), p. 453.
[39]M. E. Rose, *Elementary Theory of Angular Momentum* (Wiley, New York, 1957).
[40]*Handbook of Mathematical Functions,* edited by M. Abramowitz and I. A. Stegun (U.S. Department of Commerce, Washington, D.C., 1972).
[41]W. Kolos and L. Wolniewicz, J. Chem. Phys. **43**, 2429 (1965).
[42]W. Kolos and L. Wolniewicz, J. Chem. Phys. **45**, 509 (1966).
[43]R. J. Spindler, Jr., J. Quant. Spectrosc. Radiat. Transfer **9**, 1041 (1969).
[44]N. C. Blais and D. G. Truhlar, J. Chem. Phys. **65**, 5335 (1977).
[45]L. Wolniewicz, J. Chem. Phys. **51**, 5002 (1969).
[46]A. L. Ford, J. C. Browne, E. J. Shipsey, and P. DeVries, J. Chem. Phys. **63**, 362 (1975).
[47]J. W. Cooley, Math. Comput. **15**, 363 (1961).
[48]B. C. Garrett, L. T. Redmon, C. W. McCurdy, and M. J. Redmon, following paper, Phys. Rev. A **32**, 3366 (1985).
[49]D. W. Schwenke, G. Staszewska, and D. G. Truhlar, J. Chem. Phys. **78**, 275 (1983).
[50]M. Allan and S. F. Wong, Phys. Rev. Lett. **41**, 1791 (1978).
[51]J. M. Wadehra and J. N. Bardsley, Phys. Rev. Lett. **41**, 1795 (1978).
[52]B. C. Garrett, L. T. Redmon, and M. J. Redmon (unpublished).
[53]M. J. Redmon, B. C. Garrett, and L. T. Redmon (unpublished).